

## Single-photon electroluminescence for on-chip quantum networks

C. Bentham, D. Hallett, N. Prtljaga, B. Royall, D. Vaitiekus, R. J. Coles, E. Clarke, A. M. Fox, M. S. Skolnick, I. E. Itskevich, and L. R. Wilson

Citation: [Applied Physics Letters](#) **109**, 161101 (2016); doi: 10.1063/1.4965295

View online: <http://dx.doi.org/10.1063/1.4965295>

View Table of Contents: <http://scitation.aip.org/content/aip/journal/apl/109/16?ver=pdfcov>

Published by the [AIP Publishing](#)

---

### Articles you may be interested in

[On-chip interference of single photons from an embedded quantum dot and an external laser](#)

*Appl. Phys. Lett.* **108**, 251101 (2016); 10.1063/1.4954220

[On-chip beamsplitter operation on single photons from quasi-resonantly excited quantum dots embedded in GaAs rib waveguides](#)

*Appl. Phys. Lett.* **107**, 021101 (2015); 10.1063/1.4926729

[On-chip electrically controlled routing of photons from a single quantum dot](#)

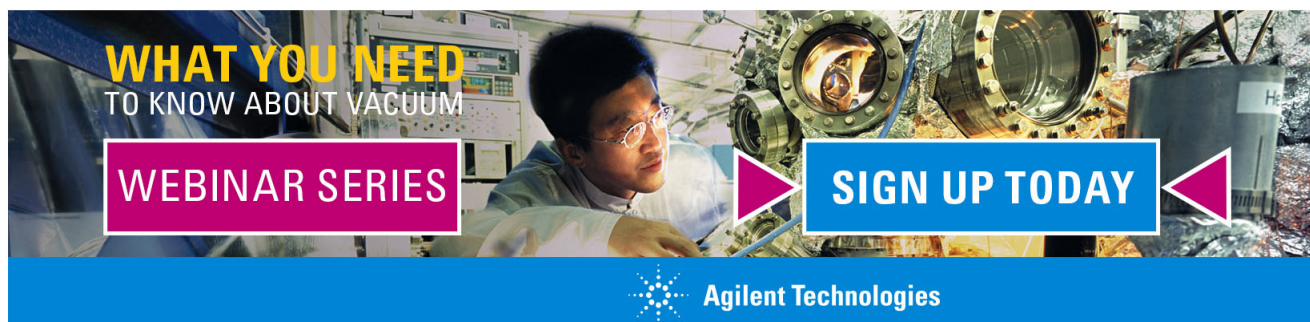
*Appl. Phys. Lett.* **106**, 221101 (2015); 10.1063/1.4922041

[Monolithic integration of a quantum emitter with a compact on-chip beam-splitter](#)

*Appl. Phys. Lett.* **104**, 231107 (2014); 10.1063/1.4883374

[APL Photonics](#)


---

A promotional banner for a webinar series. The background shows a person in a lab coat working with a large piece of scientific equipment. The text is overlaid on the image. On the left, it says 'WHAT YOU NEED TO KNOW ABOUT VACUUM' in yellow and white. Below that is a purple box with 'WEBINAR SERIES' in white. In the center, there are two purple triangles pointing towards each other. On the right, there is a blue box with 'SIGN UP TODAY' in white. At the bottom, the Agilent Technologies logo and name are displayed on a blue background.

**WHAT YOU NEED  
TO KNOW ABOUT VACUUM**

**WEBINAR SERIES**

**SIGN UP TODAY**

 **Agilent Technologies**

## Single-photon electroluminescence for on-chip quantum networks

C. Bentham,<sup>1</sup> D. Hallett,<sup>1</sup> N. Prtljaga,<sup>1</sup> B. Royall,<sup>1</sup> D. Vaitiekus,<sup>1</sup> R. J. Coles,<sup>1</sup> E. Clarke,<sup>2</sup> A. M. Fox,<sup>1</sup> M. S. Skolnick,<sup>1</sup> I. E. Itskevich,<sup>3,a)</sup> and L. R. Wilson<sup>1</sup>

<sup>1</sup>Department of Physics and Astronomy, University of Sheffield, Sheffield S3 7RH, United Kingdom

<sup>2</sup>Department of Electronic and Electrical Engineering, University of Sheffield, Sheffield S1 3JD, United Kingdom

<sup>3</sup>School of Engineering and Computer Science, University of Hull, Hull HU6 7RX, United Kingdom

(Received 24 August 2016; accepted 5 October 2016; published online 17 October 2016)

An electrically driven single-photon source has been monolithically integrated with nano-photonic circuitry. Electroluminescent emission from a single InAs/GaAs quantum dot (QD) is channelled through a suspended nanobeam waveguide. The emission line has a linewidth of below  $6 \mu\text{eV}$ , demonstrating the ability to have a high coherence, electrically driven, waveguide coupled QD source. The single-photon nature of the emission is verified by  $g^{(2)}(\tau)$  correlation measurements. Moreover, in a cross-correlation experiment, with emission collected from the two ends of the waveguide, the emission and propagation of single photons from the *same* QD is confirmed. This work provides the basis for the development of electrically driven on-chip single-photon sources, which can be readily coupled to waveguide filters, directional couplers, phase shifters, and other elements of quantum photonic networks. © 2016 Author(s). All article content, except where otherwise noted, is licensed under a Creative Commons Attribution (CC BY) license (<http://creativecommons.org/licenses/by/4.0/>). [<http://dx.doi.org/10.1063/1.4965295>]

The use of single-photons as flying qubits in quantum networks<sup>1</sup> provides a platform for quantum computation<sup>2</sup> and the secure transfer of information<sup>3</sup> in scalable optical quantum information systems.<sup>4,5</sup> For real-world applications, high component densities are likely to be required,<sup>6</sup> which can be achieved using integrated semiconductor nano-photonic circuits. In addition, integrated optical circuits are inherently stable and dramatically reduce the experimental complexity.<sup>7</sup> A key requirement for this approach is a controllable on-chip single photon source with favourable coherence properties. Moreover, if the source can be driven electrically, this provides an important advantage in terms of scalability.

Embedded semiconductor quantum dots (QDs) are very promising as on-chip light sources. Emission from single QDs has been demonstrated with both optical<sup>8–11</sup> and electrical excitation,<sup>12</sup> and the single-photon nature of the emission<sup>13–17</sup> has been established. The integration of QDs with circuit elements, such as waveguides<sup>18–20</sup> and beamsplitters,<sup>21,22</sup> has also been demonstrated. However, all experiments on integrated single-photon sources so far have relied on the external optical excitation. Although this has the benefit of limiting the emission to QDs within the excitation spot, such an approach becomes increasingly challenging for the networks requiring multiple single-photon sources. By contrast, electrical injection is a viable method of creating a true on-chip source of single photons. However, to limit the number of emitting QDs in this case provides a major challenge.

In this Letter, we demonstrate the on-chip spatially selective electrical generation of single photons and their coupling into a suspended nanobeam waveguide. The photons are generated by electrical injection into the self-assembled QDs.

Emission from only a few QDs located within a small area at the end of the waveguide, where coupling to the waveguide mode is strong, is used to produce a waveguide-coupled single-photon electroluminescence (EL) source. Our results show high photon coherence values comparable with the best reported for diode structures,<sup>23,24</sup> suggesting that the proximity of the doped layers and surfaces in the present devices does not necessarily have a significant impact on the device performance under EL conditions.

The devices are fabricated from a *p-i-n* diode structure containing a layer of self-assembled QDs. The sample was grown using molecular beam epitaxy (MBE) on an undoped (100) GaAs substrate. A 160 nm thick *p-i-n* structure was grown on the top of a 1  $\mu\text{m}$  thick  $\text{Al}_{0.6}\text{Ga}_{0.4}\text{As}$  sacrificial layer. A layer of InAs self-assembled QDs was grown in the middle of the diode using the In-flush techniques<sup>25,26</sup> with a GaAs partial cap height of 2.5 nm and density below  $10^{10} \text{cm}^{-2}$ . The dot layer is sandwiched between 50 nm GaAs spacer layers and a 30 nm Be-doped *p*-type layer on the top and a 30 nm Si-doped *n*-type layer at the bottom of the diode structure. A combination of several electron beam lithography (EBL) steps, wet etching, and inductively coupled plasma (ICP) etching was used to define the devices and provide top contacts to the *p*- and *n*-doped layers. The free standing waveguide structures were produced by selectively etching the  $\text{Al}_{0.6}\text{Ga}_{0.4}\text{As}$  sacrificial layer with hydrofluoric acid.

Figures 1(a) and 1(b), which present the device schematic and a top view scanning electron microscope (SEM) image of a typical device, respectively, illustrate the design. It consists of an electrically contacted bar (horizontal on the SEM image) running perpendicular to three suspended waveguides. Semi-circular air/GaAs grating output couplers<sup>27</sup> at the opposite end of the waveguides scatter light into the detection apparatus. The 15  $\mu\text{m}$  long waveguides have a

<sup>a)</sup>Author to whom correspondence should be addressed. Electronic mail: [i.itskevich@hull.ac.uk](mailto:i.itskevich@hull.ac.uk)



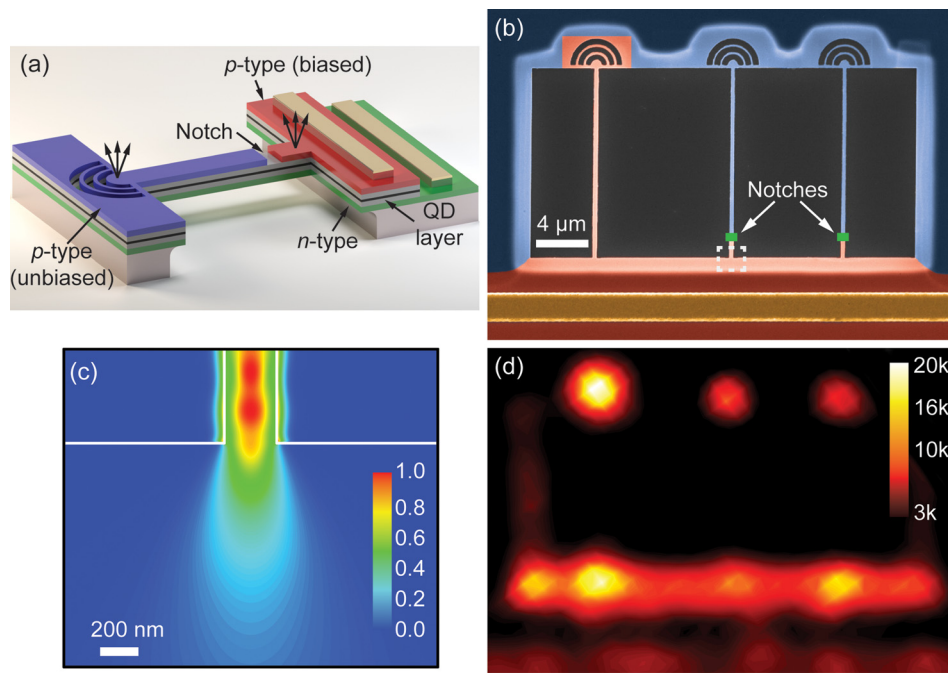


FIG. 1. (a) Device schematic. (Only one of the three waveguides is shown.) Red and blue colours represent biased and unbiased regions of the sample, respectively, separated by a notch which breaks the electrical connection in the waveguide. The gold bars represent the top electrical contacts to the  $p$ - and  $n$ -doped layers. Vertical arrows on the left- and right-hand sides of the waveguide denote the EL emission collected above the outcoupler and above the QD position, respectively. (b) The top view false colour SEM image of a typical device. The red, blue, and gold colours show the biased and unbiased regions and the top  $p$ -type contact, respectively, in the same way as in (a). Two thick green bars represent the notches. (c) Electric field intensity profile (normalised to the maximum intensity) of the waveguide mode in the QD plane, obtained by finite-difference time-domain modelling using an eigenmode source within the waveguide. The area of the figure corresponds to the dashed white square on the SEM image in (b). (d) Spectrally unfiltered EL map obtained by raster scanning the collection from the tested device, to the same scale as (b), with units of single-photon avalanche diode counts per second.

height of 160 nm (which is the thickness of the  $p$ - $i$ - $n$  structure) and a width of 290 nm; the dimensions were chosen to ensure a single-mode operation in transverse-electric (TE) polarisation. The electrical connection across the device is broken by a masked etch through the top  $p$ -type contact layer, including 30 nm deep notches [see Figure 1(b)] across two of the three waveguides (the third waveguide is used as a control). This is done to limit the EL emission to the area at the bottom edge [on the SEM image, Figure 1(b)] of the two waveguides and to prevent emission from the remaining part of the device; in particular, the notches prevent emission from most of the area of the two waveguides (i.e., the middle and the right-hand ones) and from the out-couplers.

Figure 1(c) illustrates how the propagation of EL down a waveguide from only a single or a few QDs is achieved. It shows the simulated electric field intensity profile of the optical mode, which interfaces the waveguide and membrane. It was obtained by directly exciting the waveguide mode with an eigenmode source (at 922 nm) and monitoring the electric field intensity in the QD plane.<sup>28</sup> The electric field intensity at a given point is a measure of the coupling strength of the emission of the QD at that location to the mode. Over the QD ensemble emission range, 900–950 nm, the group velocity dispersion and, therefore, the spatial shape of the mode are essentially constant. (Previous simulations<sup>20</sup> have found the group index of the mode to vary by not more than 3% in this range.) In the vertical direction, the mode spatial profile has a single antinode in the centre of the waveguide (i.e., where the QD layer is located), as expected for a fundamental mode in a rectangular waveguide. Figure 1(c) shows that

the coupling is efficient only for QDs either within the waveguide or close to the bottom edge of the waveguide, and rapidly diminishes as the emitter is moved further from the waveguide. With a notch across the waveguide, which provides an electrical break, an effective excitation area of approximately  $0.5 \mu\text{m}^2$  can be expected.

The coupling efficiency between the QD and the waveguide is an important figure of merit. Our simulations show that for an optimally positioned QD (i.e., at the electric field maximum in the centre of the waveguide), 47%–48% coupling to the mode propagating towards the outcoupler can be achieved, in agreement with Ref. 20. The value is close to the upper limit of 50% (with the remaining 50% of the emission coupling to the mode which propagates in the opposite direction). Moreover, for the QDs located at the interface between the waveguides and the electrically contacted bar (i.e., not at the maximum of the electric field within the waveguide), the coupling is only slightly lower at 45%. This demonstrates that for a single QD located within the effective excitation area, efficient coupling to the waveguide is expected.

Optical measurements were performed in a confocal microscope system, with the sample and collection lens (NA of 0.55) at 4.2 K in a helium exchange gas cryostat. The system allowed out-of-plane collection from the two spatially separated locations into two independent single mode fibres. The EL spectra were recorded using a single 0.75 m spectrometer and liquid  $\text{N}_2$  cooled charge-coupled device (CCD) camera with the resolution of  $17 \mu\text{eV}$ . High resolution EL spectra were taken using a scanning Fabry-Perot interferometer with

$0.3 \mu\text{eV}$  resolution, after initial filtering with a spectrometer. For time-correlated single-photon counting measurements, the emission was filtered using two separate  $0.75 \text{ m}$  spectrometers with a bandwidth of  $90 \mu\text{eV}$  and detected by two single-photon avalanche diodes (SPADs).

Figure 1(d) shows an EL map, which was obtained by raster scanning the collection across the device using motorised mirrors, while recording the integrated intensity on a SPAD. The scan area matches the SEM image shown in Fig. 1(b), with the control waveguide on the left-hand side. Emission is only observed from the electrically active regions and out-couplers. The out-couplers are bright due to coupling of the EL emission from the QDs in the contacted regions to the waveguides. Brighter spots at the interface between the waveguides and the electrically contacted bar appear due to light scattering. The map confirms the design performance of the waveguides and verifies the electrical isolation. Current-voltage characteristics of the devices (not shown) demonstrate typical diode behaviour, with turn-on voltage around  $1.4 \text{ V}$ .

Figure 2 presents the EL spectra from a typical device, collected separately from each end of a waveguide (i.e., vertically above the emitting QDs and at the out-coupler). The onset of predominantly single-dot EL emission occurs at  $2.3\text{--}2.4 \text{ V}$ , as shown in Fig. 2(b).<sup>29</sup> With bias, the lines grow in intensity. At approximately  $2.9 \text{ V}$ , the background emission also starts increasing, which can most likely be attributed to EL from other QDs, and becomes increasingly strong with increasing voltage as seen in Fig. 2(d). A bright line is observed in all spectra at  $921.8 \text{ nm}$ . We argue later that it is an emission line from the same QD, both in the spectra collected above the QD and from the out-coupler. The best

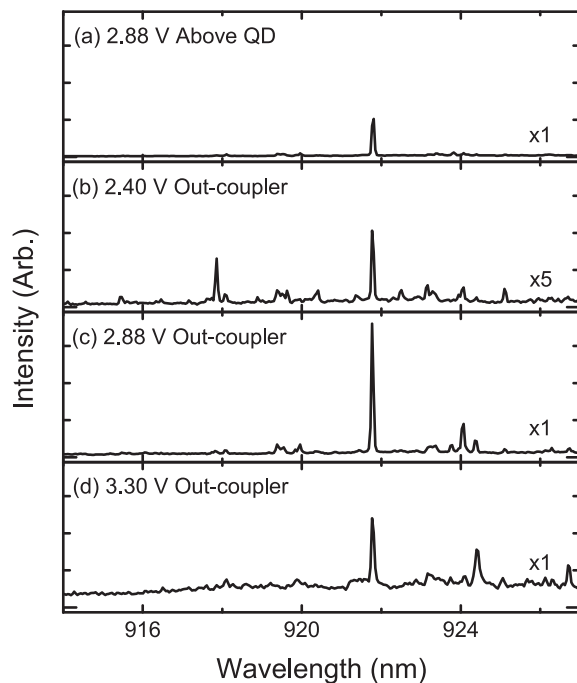


FIG. 2. Electroluminescence spectra collected from (a) above the QD at a bias of  $2.88 \text{ V}$  and from the out-coupler at a bias of (b)  $2.40 \text{ V}$ , (c)  $2.88 \text{ V}$ , and (d)  $3.30 \text{ V}$ . The line at  $921.8 \text{ nm}$  is observed in the spectra from both above the dot and from the out-coupler, demonstrating the propagation of single-dot EL down the waveguide.

signal-to-background ratio for this line is achieved at  $2.88 \text{ V}$ . At this bias, the line intensity (measured on the CCD) in the spectra collected above the QD and from the out-coupler is as high as  $30\,000$  and  $80\,000$  counts/s, respectively, which is indicative of efficient coupling of the dot to the waveguide mode. These spectra are shown in Figs. 2(a) and 2(c).

All further investigations were performed using the emission line at  $921.8 \text{ nm}$  at  $2.88 \text{ V}$ . In the previous spectra, its linewidth is limited by the spectrometer resolution. To achieve higher resolution, the EL spectra were taken using a Fabry-Perot interferometer, collected from the out-coupler. These spectra, shown in Fig. 3, reveal that the line is a doublet with a linewidth of  $5.9 \mu\text{eV}$  and a splitting of  $15 \mu\text{eV}$ . The doublet is most likely to be due to fine structure splitting (FSS) of the neutral exciton state. The measured linewidth, which remains constant from EL onset to  $2.9 \text{ V}$ , is comparable to the best reported values for *p-i-n* diode samples, such as for EL emission in thicker structures,  $400 \text{ ps}$  ( $3.3 \mu\text{eV}$ ),<sup>23</sup> and resonance fluorescence in membrane devices under reverse bias,  $0.62 \text{ GHz}$  ( $2.6 \mu\text{eV}$ ).<sup>24</sup> At higher bias, the linewidth increases with the rising background in agreement with Ref. 23, in which it was attributed to charge noise fluctuations. The observation of narrow linewidth EL is also in agreement with the suggestion that applied electric fields can stabilise the charge environment of quantum dots.<sup>30</sup> Altogether, this result demonstrates that high coherence, electrically excited emission can be achieved from QDs incorporated in thin photonic diode structures.

The single-photon nature of the QD source was verified with a Hanbury Brown and Twiss (HBT) experiment, in which the filtered emission collected above the QD was passed through a fibre beam splitter, and coincidences were recorded. The resulting normalised histogram for the second order correlation function  $g^{(2)}(t)$  without background subtraction is shown in Fig. 4(a). A raw value  $g_{\text{raw}}^{(2)}(0) = 0.34 \pm 0.04$  was measured. By deconvolving the experimental data with the temporal response of the detection system (Gaussian, full width at half maximum of  $870 \text{ ps}$ ),  $g^{(2)}(0) = 0.10 \pm 0.03$  was obtained, which shows that the source is

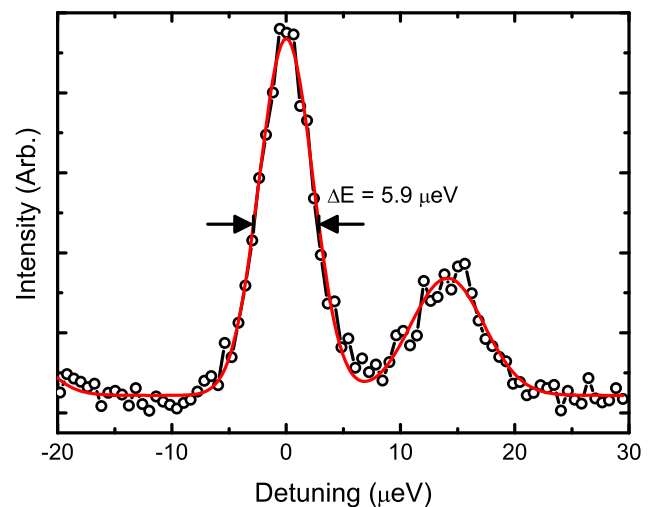


FIG. 3. The high-resolution spectrum of the investigated emission line (open black circles) at  $2.88 \text{ V}$  obtained by Fabry-Perot interferometry. Red continuous line shows a fit to the data. The doublet structure very likely arises from fine-structure splitting.

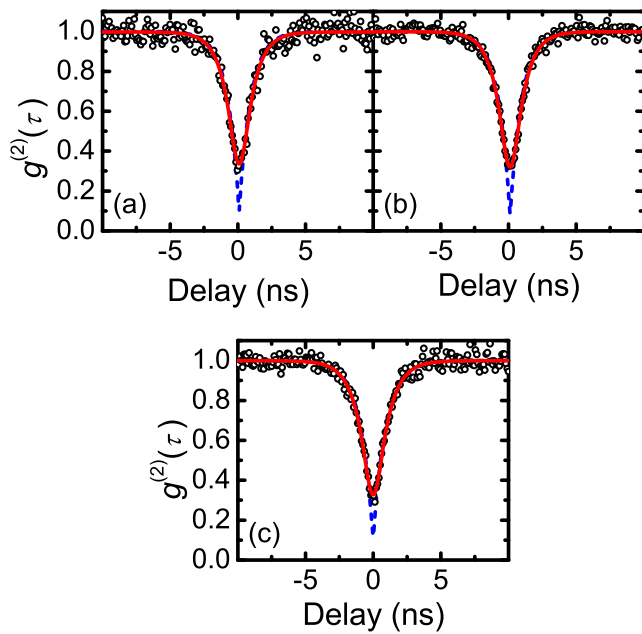


FIG. 4. Normalised second order correlation function for the quantum dot (a) measured at the QD location, (b) measured at the out-coupler, and (c) cross correlated between photons collected at the out-coupler and at the QD location. In each plot, open black circles are the experimental data, continuous red line is a fit to the raw data, and dashed blue line corresponds to a fit in the limit of an infinitely fast detector.

strongly antibunched. The remaining multi-photon emission probability is likely to be due to the residual background emission that can be seen in Fig. 2(a).

The propagation of single-photons along the waveguide was confirmed with an HBT experiment with the emission collected from the out-coupler. Raw and deconvolved values  $g_{raw}^{(2)}(0) = 0.32 \pm 0.03$  and  $g^{(2)}(0) = 0.07 \pm 0.02$  were obtained, as shown in Fig. 4(b). Again, the emission is strongly antibunched, demonstrating that it passes through the waveguide without the deterioration of the photon statistics.

To verify the origin of the line, a cross-correlation measurement was performed, in which correlations were recorded between the emission collected above the QD and from the out-coupler. The resulting normalised histogram is presented in Fig. 4(c). Raw and deconvolved values are  $g_{raw}^{(2)}(0) = 0.33 \pm 0.03$  and  $g^{(2)}(0) = 0.10 \pm 0.02$ . This unambiguously proves that the emission observed at both ends of the waveguide originates from the same QD, i.e., that the single-photon EL emission from a single quantum dot couples to the waveguide mode and propagates along the waveguide.

In conclusion, we have demonstrated the monolithic integration of an on-demand electrically driven high quality quantum emitter, a single InAs self-assembled quantum dot, with a nanobeam waveguide. With careful design and fabrication, we are able to electrically excite and direct the highly coherent single-photon emission from a single quantum dot along the waveguide. This proof of concept device provides the basis for practical on-chip electrically driven single-photon sources, which can be readily coupled to waveguide filters, directional couplers, and other elements of quantum photonic networks.

This work was funded by EPSRC Grant No. EP/J007544/1.

- <sup>1</sup>H. J. Kimble, *Nature* **453**, 1023 (2008).
- <sup>2</sup>T. D. Ladd, F. Jelezko, R. Laflamme, Y. Nakamura, C. Monroe, and J. L. O'Brien, *Nature* **464**, 45 (2010).
- <sup>3</sup>N. Gisin, G. Ribordy, W. Tittel, and H. Zbinden, *Rev. Mod. Phys.* **74**, 145 (2002).
- <sup>4</sup>E. Knill, R. Laflamme, and G. J. Milburn, *Nature* **409**, 46 (2001).
- <sup>5</sup>M. A. Nielsen, *Phys. Rev. Lett.* **93**, 40503 (2004).
- <sup>6</sup>J. L. O'Brien, A. Furusawa, and J. Vučković, *Nat. Photonics* **3**, 687 (2009).
- <sup>7</sup>S. Tanzilli, A. Martin, F. Kaiser, M. P. De Micheli, O. Alibart, and D. B. Ostrowsky, *Laser Photonics Rev.* **6**, 115 (2012).
- <sup>8</sup>J.-Y. Marzin, J.-M. Gérard, A. Izraël, D. Barrier, and G. Bastard, *Phys. Rev. Lett.* **73**, 716 (1994).
- <sup>9</sup>E. Dekel, D. Gershoni, E. Ehrenfreund, D. Spektor, J. M. Garcia, and P. M. Petroff, *Phys. Rev. Lett.* **80**, 4991 (1998).
- <sup>10</sup>Y. Toda, S. Shinomori, K. Suzuki, and Y. Arakawa, *Appl. Phys. Lett.* **73**, 517 (1998).
- <sup>11</sup>A. Kuther, M. Bayer, A. Forchel, A. Gorbunov, V. B. Timofeev, F. Schäfer, and J. P. Reithmaier, *Phys. Rev. B* **58**, R7508 (1998).
- <sup>12</sup>I. E. Itskevich, S. I. Rybchenko, I. I. Tartakovskii, S. T. Stoddart, A. Levin, P. C. Main, L. Eaves, M. Henini, and S. Parnell, *Appl. Phys. Lett.* **76**, 3932 (2000).
- <sup>13</sup>P. Michler, A. Kiraz, C. Becher, W. V. Schoenfeld, P. M. Petroff, L. Zhang, E. Hu, and A. Imamoglu, *Science* **290**, 2282 (2000).
- <sup>14</sup>S. Strauf, N. G. Stoltz, M. T. Rakher, L. A. Coldren, P. M. Petroff, and D. Bouwmeester, *Nat. Photonics* **1**, 704 (2007).
- <sup>15</sup>W.-H. Chang, W.-Y. Chen, H.-S. Chang, T.-P. Hsieh, J.-I. Chyi, and T.-M. Hsu, *Phys. Rev. Lett.* **96**, 117401 (2006).
- <sup>16</sup>M. Pelton, C. Santori, J. Vučković, B. Zhang, G. S. Solomon, J. Plant, and Y. Yamamoto, *Phys. Rev. Lett.* **89**, 233602 (2002).
- <sup>17</sup>Z. Yuan, B. E. Kardynal, R. M. Stevenson, A. J. Shields, C. J. Lobo, K. Cooper, N. S. Beattie, D. A. Ritchie, and M. Pepper, *Science* **295**, 102 (2002).
- <sup>18</sup>A. Schwagmann, S. Kalliakos, I. Farrer, J. P. Griffiths, G. A. Jones, D. A. Ritchie, and A. J. Shields, *Appl. Phys. Lett.* **99**, 261108 (2011).
- <sup>19</sup>S. Kalliakos, Y. Brody, A. Schwagmann, A. J. Bennett, M. B. Ward, D. J. P. Ellis, J. Skiba-Szymanska, I. Farrer, J. P. Griffiths, G. A. C. Jones, D. A. Ritchie, and A. J. Shields, *Appl. Phys. Lett.* **104**, 221109 (2014).
- <sup>20</sup>M. N. Makhonin, J. E. Dixon, R. J. Coles, B. Royall, I. J. Luxmoore, E. Clarke, M. Hugues, M. S. Skolnick, and A. M. Fox, *Nano Lett.* **14**, 6997 (2014).
- <sup>21</sup>N. Prtljaga, R. J. Coles, J. O'Hara, B. Royall, E. Clarke, A. M. Fox, and M. S. Skolnick, *Appl. Phys. Lett.* **104**, 231107 (2014).
- <sup>22</sup>N. Prtljaga, C. Bentham, J. O'Hara, B. Royall, E. Clarke, L. R. Wilson, M. S. Skolnick, and A. M. Fox, *Appl. Phys. Lett.* **108**, 251101 (2016).
- <sup>23</sup>R. B. Patel, A. J. Bennett, K. Cooper, P. Atkinson, C. A. Nicoll, D. A. Ritchie, and A. J. Shields, *Phys. Rev. Lett.* **100**, 207405 (2008).
- <sup>24</sup>D. Pinotsi, P. Fallahi, J. Miguel-Sanchez, and A. Imamoglu, *IEEE J. Quantum Electron.* **47**, 1371 (2011).
- <sup>25</sup>S. Fafard, Z. Wasilewski, C. Allen, D. Picard, M. Spanner, J. McCaffrey, and P. Piva, *Phys. Rev. B* **59**, 15368 (1999).
- <sup>26</sup>Z. R. Wasilewski, S. Fafard, and J. P. McCaffrey, *J. Cryst. Growth* **201**, 1131 (1999).
- <sup>27</sup>A. Faraon, I. Fushman, D. Englund, N. Stoltz, P. Petroff, and J. Vučković, *Opt. Express* **16**, 12154 (2008).
- <sup>28</sup>Lumerical Solutions, Inc., see <http://www.lumerical.com/tcad-products/fdtd/> for A commercial-grade simulator based on the finite-difference time-domain method was used to perform the calculations.
- <sup>29</sup>In our device, we have a significant series resistance; due to that, 2.3–2.4 V is not the value of the voltage drop across the *p-i-n* diode, which is significantly lower.
- <sup>30</sup>N. Somaschi, V. Giesz, L. De Santis, J. C. Loredó, M. P. Almeida, G. Hornecker, S. L. Portalupi, T. Grange, C. Antón, J. Demory, C. Gómez, I. Sagnes, N. D. Lanzillotti-Kimura, A. Lemaître, A. Auffeves, A. G. White, L. Lanco, and P. Senellart, *Nat. Photonics* **10**, 340 (2016).